Large Reductions in Satellite-Derived and Modelled European Lower Tropospheric Ozone During and After the COVID-19 Pandemic (2020–2022)

Matilda. A. Pimlott[1], Richard. J. Pope[1,2], Brian. J. Kerridge[3,4], Richard. Siddans[3,4], Barry. G. Latter[3,4], Lucy. J. Ventress[3,4], Wuhu. Feng[1,5], Martyn. P. Chipperfield[1,2]

[1]School of Earth and Environment, University of Leeds, Leeds, LS2 9JT, UK

[2]National Centre for Earth Observation, University of Leeds, Leeds, LS2 9JT, UK

[3]Remote Sensing Group, STFC Rutherford Appleton Laboratory, Chilton, Oxfordshire, OX11 0QX, UK

[4]National Centre for Earth Observation, STFC Rutherford Appleton Laboratory, Chilton, Oxfordshire, OX11 0QX, UK

[5]National Centre for Atmospheric Science, University of Leeds, Leeds, LS2 9PH, UK

Submitted to *Atmospheric Chemistry and Physics*

Corresponding author: Richard J. Pope (R.J.Pope@leeds.ac.uk)

Key Points:

- The European satellite record shows large lower tropospheric spring-summer ozone reductions in 2020–2022 (8.4-14.6%).~~, of 11.0%, 8.4% and 14.6%.~~
- Scaling precursor emissions based on activity data yields large model ozone reductions in the spring-summer of 2020 and 2021.
- In 2020, meteorology contributed ~1/3 of the modelled reduction (low stratosphere-troposphere flux), with ~2/3 from emission reductions.

Abstract

Activity restrictions during the COVID-19 pandemic caused large-scale reductions in ozone (O_3) precursor emissions, which in turn substantially reduced the abundance of tropospheric O_3 in the Northern Hemisphere. Satellite records of lower tropospheric column O_3 (0 – 6 km) from the Rutherford Appleton Laboratory (RAL) highlight these large reductions in O_3 during the COVID-19 period (2020), which persisted into 2021 and 2022. The European domain average O_3 reduction ranged between 2.0 and 3.0 Dobson units (DU) (11.0-14.6%). These satellite results were supported by the TOMCAT chemistry transport model (CTM) through several model sensitivity experiments to account for changes in emissions and impact of the meteorological conditions in 2020. Here, the business-as-usual (BAU) emissions were scaled by activity data (i.e. anonymised mobility data from big tech companies) to account for the reduction in O_3 precursor emissions. The model simulated large O_3 reductions (2.0-3.0 DU), similar to the satellite records, where approximately 66% and 34% of the O_3 loss can be explained by emissions changes and meteorological conditions, respectively. Our results also show that the reduced flux of stratospheric O_3 into the troposphere accounted for a substantial component of the meteorological signal in the overall lower tropospheric O_3 levels during the COVID-19 period.~~Activity restrictions during the COVID-19 pandemic caused large reductions in ozone (O_3) precursor emissions. Studies showed large O_3 reductions in the 2020 spring-summer Northern Hemisphere free troposphere coinciding with this emission reduction period. Here, we provide an insight into the European satellite-derived tropospheric O_3 record updated to mid-2023. Rutherford Appleton Laboratory (RAL) retrieval products show large negative anomalies in the spring-summer periods of 2020 – 2022, with the largest in 2022, and smaller reductions in 2023. The Infrared Atmospheric Sounding Interferometer (IASI) showed peak reductions compared to monthly averages of 2.2 DU (11.0%), 1.7 DU (8.4%) and 2.8 DU (14.6%) in 2020, 2021 and 2022, respectively. Scaling model emissions, based on activity reduction data, yields large negative anomalies peaking in May 2020 and 2021. Emissions reduction was the greater influence, explaining ~65% of the decrease, however, the meteorological impact was substantial, driven by a reduced stratosphere-troposphere O_3 exchange flux.~~

Plain Language Summary

Lockdowns and other measures implemented to limit the spread of COVID-19 reduced human activity, leading to a reduction in emissions from humans, including precursors for tropospheric ozone (O_3), a pollutant and greenhouse gas. Studies have shown a reduction in tropospheric O_3 across the northern hemisphere in the spring-summer of 2020, which coincided with this emission reduction. We provide further evidence of the tropospheric O_3 reduction in 2020, specifically for Europe, using two records derived from satellite instruments. The two records show large reductions in European tropospheric O_3 in the spring-summer of 2020, peaking at ~ 10 – 20 % in May. ~~One record continues into 2023, showing the largest reductions in 2022, the year after the initial 2020/2021 pandemic period, however, the reductions are smaller in the following year of 2023.~~ We use a chemical transport model to distinguish between the impacts of emissions and meteorology in 2020–2021. In both years, emission reductions had greater influence on the O_3 reduction (~2/3), highlighting the importance of emissions in decreasing O_3. However, emissions reductions alone were not responsible for the large O_3 reduction, as there was considerable influence from meteorology (~1/3), mostly from variation in the flux of O_3 from the stratosphere.

Formatted: Font: 10 pt

Formatted: Font: (Default) Times New Roman, 10 pt

Formatted: Font: 10 pt

1 Introduction

Tropospheric O_3 is an important secondary atmospheric pollutant and short-lived climate forcer, formed in the presence of the precursor gases, nitrogen oxides (NO_x, referring to nitrogen dioxide (NO_2) and nitric oxide (NO)) and volatile organic compounds (VOCs), and sunlight (P. S. Monks et al., 2015). Tropospheric O_3 is a persistent health problem in Europe, with 24,000 premature deaths attributed to acute O_3 exposure in 2020 (European Environment Agency, 2022). O_3 is also the 3rd most important greenhouse gas, with an estimated effective radiative forcing of 0.47 W m^{-2} (0.24–0.71 W m^{-2}) between 1750–2019, dominated by changes in tropospheric O_3 (IPCC, 2021; Skeie et al., 2020).

Due to a global pandemic caused by COVID-19 (disease from SARS-CoV-2, severe acute respiratory syndrome coronavirus-2), many countries worldwide implemented a 'lockdown' of daily life activities to prevent the spread of the disease (Forster et al., 2020; WHO, 2020; Zhou et al., 2020). This resulted in a widespread reduction in anthropogenic surface emissions, including O_3 precursor gases. Based on activity data, Forster et al. (2020) estimated a global reduction of ~ 30% for NO_x, 25% for carbon monoxide (CO) and 20% for VOCs in April 2020 and Guevara et al. (2021) estimated reductions of ~ 33% for NO_x and 8% for VOCs in March/April 2020. Here, the changes in activity data reported by Forster et al., (2020) are based on changes in anonymised mobility data (e.g. from phone GPS information) provided by Apple and Google (see Forster et al., (2020) and references within). Typically, they found these mobility datasets used in their study to be within 20% of each other and had a correlation of 0.8 or higher. Furthermore, Guevara et al. (2021) found that countries with the severest lockdowns had even higher average reductions (~ 50% for NO_x, 14% for VOCs).

Reductions in tropospheric O_3 in the spring-summer across the northern hemisphere (NH) free troposphere (FT) was initially described by Steinbrecht et al. (2021). The timing of this reduction coincides with the introduction of lockdowns across Europe, beginning in the spring-summer of 2020 and continuing into 2021. Steinbrecht et al. (2021) found that in 2020, measurements of the NH FT (mostly from ozonesondes) from April–August showed ~7% lower O_3 values, compared to its climatology of 2000–2020. Such a widespread reduction occurring at so many stations had not occurred previously in this time period. Another notable event during winter-spring of 2019/2020 was the very large stratospheric Arctic O_3 depletion caused by a very cold, strong and long-lasting polar vortex (W. Feng et al., 2021; Weber et al., 2021; Wohltmann et al., 2020). Steinbrecht et al. (2021) suggested that this low stratospheric O_3 event contributed to less than 25% of this O_3 negative anomaly, attributing most of the O_3 reduction to emission reductions. Further studies have confirmed low FT O_3 across Europe and the NH using aircraft and ozonesonde measurements (e.g. Chang et al. (2022); Clark et al. (2021); Putero et al. (2023). In contrast, Parrish et al. (2022) suggested that low 2020 tropospheric O_3 could be largely due to a negative trend in baseline tropospheric O_3 since around the mid-2010s, based on Western European surface sites.

From a satellite perspective, Ziemke et al. (2022) found low NH spring-summer FT O_3 from instruments aboard NASA satellites, using a merged instrument record. The tropospheric column O_3 reduction of ~ 7–8% (3 DU)

Formatted: Font: 10 pt

Formatted: Font: (Default) Times New Roman, 10 pt

Formatted: Font: (Default) Times New Roman, 10 pt

(compared to 2016–2019), was comparatively uniform between 20°N - 60°N and repeated in the next year, 2021. They found a reduction of NH satellite-derived NO_2 (~ 10–20%) in the spring-summer of 2020 and 2021, attributing this as the likely cause of the O_3 reduction. Cuesta et al. (2022) found that satellite-derived lowermost tropospheric O_3 (< 3 km altitude) in the spring (1^{st}–15^{th} April) of 2020 was enhanced across central Europe and northern Italy (typically VOC-limited regions) compared to the previous year (2019) and reduced elsewhere in Europe (typically NO_x-limited regions). An enhancement of O_3 across central Europe in the spring-summer of 2020 was also found at surface monitoring sites (e.g. Ordóñez et al. (2020); Grange et al. (2021)). Apart from Ziemke et al. (2022), there are few studies of 2021 and onwards. One example is from Pey & Cerro (2022), finding reduced background O_3 values over SW Europe (~15% at most sites) in March-April 2020, which was also seen in 2021 but to a lesser extent. Similar results were found in the study by Dunn et al., (2024).

Modelling studies have investigated the impact of emission reduction on FT O_3, using different methods to estimate the size of these emission reductions, which are still uncertain. Bouarar et al. (2021) modelled primary pollutant emission reductions, based on emission reductions from activity data by Doumbia et al. (2021), finding zonally averaged NH FT O_3 to be reduced by 5–15% (2001–2019 baseline). One third of this reduction is attributed to reductions in air traffic, one third is attributed to a reduction in surface emissions and the final third is attributed to meteorology, including the low 2020 springtime Arctic stratospheric O_3. Miyazaki et al. (2021) used data assimilation, finding a reduction in the global tropospheric O_3 burden of ~ 2% in May and June 2020.

Here, we present an update to the European tropospheric O_3 record using two satellite products, extending the record to mid-2023, and present the reductions in the lower FT compared to previous years. Using a 3-D chemical transport model, TOMCAT (S. A. Monks et al., 2017), we explore the impact of scaling the anthropogenic surface emissions (from activity data changes) on European tropospheric O_3 in 2020 and 2021. Lastly, we quantify the relative contribution of emissions and meteorology to the modelled reduction in tropospheric O_3.

2 Data and Methods

Formatted: Font: 10 pt

2.1 Tropospheric Ozone Satellite Datasets

We present satellite-derived O_3 from two satellite instruments, the Infrared Atmospheric Sounding Interferometer (IASI) and the Global Ozone Monitoring Experiment-2 (GOME-2), both aboard EUMETSAT's satellite MetOp-B (Clerbaux et al., 2009; Munro et al., 2016). The MetOp series of satellites have a sun-synchronous, near polar orbit with an equator crossing time of 9:30 local solar time (LST). IASI has a swath width of 2200 km, and in the nadir viewing mode, there are four circular fields of view across-track with a diameter of 12 km, covering a square 50 × 50 km^2 which is scanned across the swath. IASI measures in the infrared (IR) wavelengths (645–2760 cm^{-1}) with a spectral resolution of 0.3 - 0.5 cm^{-1} (Clerbaux et al., 2009). GOME-2 measures in the ultraviolet-visible (UV-Vis) wavelengths (240–790 nm) with a spectral resolution of 0.26 - 0.51 nm, and has a swath width of 1920 km. The field of view is scanned across-track yielding 24 ground-pixels of dimension 80 km (across-track) × 40 km (along-track) (Callies et al., 2000; Munro et al., 2016). For quality assurance, the GOME-2B record was filtered for a geometric

cloud fraction of <0.2 (e.g. Miles et al. (2015)) and the IASI-IMS-extended record was filtered for an effective cloud fraction of <0.5 (as in Pope et al. (2021)). Here, the RAL Space GOME-2 and IASI Infrared and Microwave Sounding (IMS) retrieval schemes for lower tropospheric ozone have been independently evaluated against ozonesonde data in Miles et al., (2015) and Pimlott et al., (2022).

Height-resolved O_3 distributions are retrieved by the Rutherford Appleton Laboratory (RAL) using the IMS-Extended scheme for IASI (detailed in Pope et al. (2021)) and UV-Vis scheme for GOME-2 (detailed in Miles et al. (2015)). Due to an underlying negative tendency in the GOME-2 record, likely from UV degradation of the instrument, we have detrended that record, as shown in **Supplement Text S1** and **Figure S1**. To compare the IASI-IMS-Extended data from MetOp-B (2018–2023) to a longer time-period, we combine the record with IASI-IMS-Extended data from MetOp-A (2008–2017). The MetOp-B record was adjusted according to monthly differences with the MetOp-A record in the overlap year of 2018, as described in **Supplement Text S2** and **Figures S2 and S3**. Here we use lower tropospheric sub-columns of the surface–450 hPa (~6 km altitude) derived from the retrieved profiles, with a focus on Europe. As such, we use a land mask to extract a terrestrial European signal given the direct link between surface O_3, precursors gases and air pollution exposure (see **Supplement Figure S4**).

2.2 Model Simulations

We use the TOMCAT 3-D chemical transport model to simulate tropospheric O_3 between 2017 and 2021. The model control simulation is for 2017, 2018 and 2019. However, in 2020, the control simulation splits into two scenarios: 1) business-as-usual scenario (BAU) and 2) scaled emission scenario (COVID). For the BAU scenario, the control modelled emissions inventory is used but for the COVID scenario, we apply emission reduction factors (Forster et al., 2020) to model surface and aircraft emissions to account for changes in activity due to the pandemic in 2020 and 2021. However, COVID scaling for emissions are not available beyond 2021, so the model simulations are restricted to 2017-2021. TOMCAT is an off-line model driven by 6-hourly ERA-5 meteorological reanalyses (e.g. temperature, relative humidity, winds; Hersbach et al., 2020), which are provided by the European Centre for Mid-Range Weather Forecasting (ECMWF). The ERA-5 meteorological reanalyses are provided on 137 vertical levels (surface to 1 hPa), which are interpolated onto the TOMCAT vertical grid (31 levels -see Monks et al., (2017) Figure 1).~~TOMCAT is an off-line model driven by 6-hourly ERA-5 meteorological reanalyses (Hersbach et al., 2020),~~ It has a horizontal ~~with~~ a resolution of 2.8° × 2.8° and 31 vertical levels between the surface and 10 hPa, coupled with the Global Model of Aerosol Processes (GLOMAP) (Chipperfield, 2006; Mann et al., 2010; Spracklen et al., 2005). The chemistry scheme includes approximately 80 advected tracers and over 200 chemical reactions (S. A. Monks et al., 2017). Surface emission fields are described in detail in **Supplement Text S4** and **Table S1**. The anthropogenic emissions are from the Coupled Model Intercomparison Project Phase 6 (CMIP6) (L. Feng et al., 2020), whereby after 2014 emissions are based on Shared Socioeconomic Pathways (SSPs) (Gidden et al., 2019; Riahi et al., 2017). In this study, we have used the middle-of-the-road scenario, SSP2-4.5, for the TOMCAT control run between 2017 and 2019, before diverging into the BAU and COVID simulations. For the BAU simulation, the CMIP6 SSP2-4.5 emissions are used but for the COVID simulation, scaling factors for emission reductions from

Formatted: Font: (Default) Times New Roman, 10 pt

Formatted: Font: 10 pt

Formatted: Font: (Default) Times New Roman, 10 pt

Formatted: Font: (Default) Times New Roman, 10 pt

national lockdowns come from Forster et al. (2020) and were applied to the BAU emissions. Forster et al. (2020) used national mobility/activity data to estimate reductions in air pollutant emissions (i.e. NO_x, CO, VOCs, black carbon (BC) and organic carbon (OC)). **Figure 1(a)** highlights the impacts of the scale factors, with substantial decreases evident in European emissions for NO_x, CO and VOCs. **Figure 1(b)** shows that the peak reductions were in April 2020, once most European lockdowns were in effect, with monthly reductions of 0.44 Tg (33%), 0.75 Tg (34%) and 0.06 Tg (29%) of NO_x (as NO_2), CO and NMVOCs (as carbon (C)), respectively. For 2020, a secondary winter emissions reduction occurs at ~ 15–20% as further European lockdowns were imposed to reduce the spread of COVID-19. For 2021, the scaling factors from Forster et al. (2020) suggest that emissions were approximately 10–13% lower than expected but remained consistent throughout the year, suggesting a potential 'new normal' of lower precursor emissions. A tracer for stratosphere-troposphere exchange (STE) in the model (O_{3S}) is used to understand the impact of O_3 transport from the stratosphere. In the stratosphere, it is set equal to the model-calculated O_3. The only tropospheric source of the tracer is transport from the stratosphere while its sinks are via photolysis, surface deposition and reactions with HO_2, OH and H_2O through $O(^1D)$ produced from O_{3S} (S. A. Monks et al., 2017). Overall, TOMCAT is a robust and well evaluated CTM having been used in multiple studies of tropospheric O_3 and compared with many types of observation (e.g. Richards et al., (2013), Pope et al., (2020) and Pope et al., (2023, 2024). The simulated tropospheric ozone burden is a common metric to assess the skill of a model to simulate tropospheric ozone. Here, we derive a tropospheric O_3 burden of 322 Tg (BAU 2020 simulation), which is consistent with that of Monks et al., (2017) who reported an equivalent of 331 Tg. Both estimates sit within the reported range of 337±23 Tg from the Atmospheric Chemistry and Climate Model Intercomparison Project (ACCMIP, Young et al., 2013) further demonstrating TOMCAT to be a suitable modelling framework. Highly relevant for this work, Pope et al., (2023) included a detailed comparison of lower tropospheric ozone between TOMCAT and GOME-2/IASI, where thorough consideration of the satellite averaging kernels (i.e. function of satellite vertical sensitivity when retrieving sub-column profiles of O_3) was taken in conjunction with the model, generally displaying good agreement with the between them. Therefore, we are confident in using TOMCAT to directly investigate the impact of COVID-19 on lower tropospheric ozone over Europe.

~~Overall, TOMCAT is a robust and well evaluated CTM having been used in multiple studies of tropospheric O_3 (e.g. Richards et al. (2013), Pope et al. (2021) and Pope et al. (2023)), thus a suitable modelling framework for this study.~~

Formatted: Font: (Default) Times New Roman, 10 pt

Formatted: Font: (Default) Times New Roman, 10 pt

Formatted: Font: (Default) Times New Roman, 10 pt

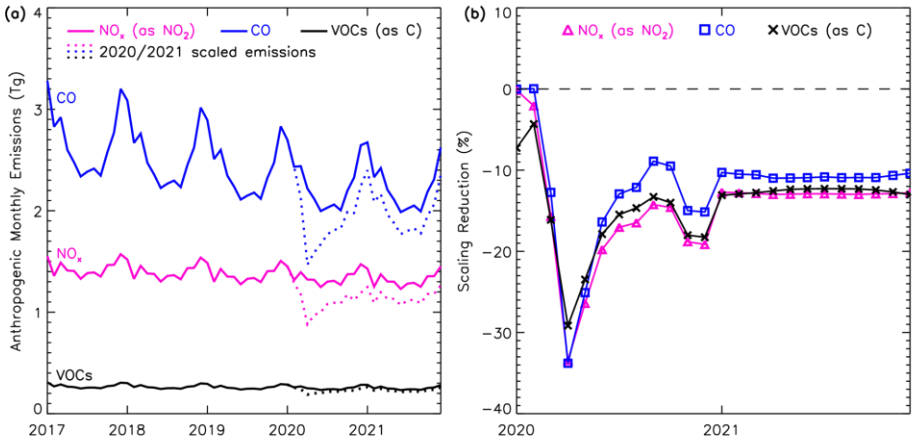

Figure 1. European aggregated anthropogenic monthly emissions of NO_x (as NO_2), CO and NMVOCs (as C) used in the TOMCAT simulations between 2017 and 2021. (a) BAU emissions (solid) and COVID emissions in 2020 and 2021 (dotted) (Tg). (b) Percentage reduction in 2020 and 2021 for NO_x, CO and VOCs in the COVID emissions, relative to the BAU emissions.

3 Results and Discussion

3.1 European Tropospheric Ozone Satellite Record (2008–2023)

We present two satellite-derived lower tropospheric sub-column O_3 records for continental Europe from 2008–2023 (**Figure 2**). During the overlapping years of 2015–2019, the records show an average difference of 2.5 DU, but the variability is well correlated (Pearson's correlation coefficient ~ 0.80). Satellite record inconsistencies are likely due to differences between IR and UV-Vis instruments, the related retrieval schemes and their vertical sensitivities, despite the instruments being aboard the same platform and having the same overpass time. Compared to a monthly baseline of 2015–2019 for GOME-2B and 2008–2019 for IASI-IMS-Extended, the monthly anomalies (**Figure 2(b)**) show good agreement through this overlap period, with the most notable disagreements in winter/spring of 2015 and spring-summer 2016. Both records show large negative anomalies in spring-summer 2020. GOME-2B shows peak negative anomalies of 2.4 DU (18.3%) and 3.0 DU (21.4%) in April and May 2020, respectively, and IASI-IMS-Extended shows slightly smaller negative anomalies of 1.7 DU (9.4%) and 2.2 DU (11.0%) in April and May, respectively. For the records shown in **Figure 2(b)**, two standard deviations (2σ) across the entire monthly record is 2.1 DU for GOME-2B and 1.8 DU for IASI-IMS-Extended. Thus, ~ 95% of the data ranges between the average ± 2σ for the respective records. In both cases, April and May 2020 negative anomalies either match or surpass this range signifying relatively substantial anomalies for these months, highlighting their unusual nature. The reductions continue into the summer of 2020, with both records showing large negative anomalies in July and

Formatted: Font: 10 pt

August: 1.7 DU (9.2%) and 1.4 DU (7.2%) for GOME-2B; 1.8 DU (8.3%) and 1.3 DU (6.3%) for IASI-IMS-Extended.

Tropospheric O_3 reductions continue into the spring and summer period of 2021, with the IASI-IMS-Extended record showing negative anomalies in most months of 2021, however, these anomalies are slightly smaller than in 2020. The largest negative anomalies are in April, May and June, at 1.0 DU (5.3%), 1.7 DU (8.4%) and 1.1 DU (5.2%), respectively, with only the reduction in May being close to the average ± 2σ threshold. This recurrence in 2021 of a tropospheric O_3 reduction of similar magnitude to 2020 is consistent with the combined NASA satellite product tropospheric column O_3 record for the 20-60N latitude band reported by Ziemke et al. (2022), which is presented from January–August.

It is worth noting that there is approximately a 1-month lag between the IASI and GOME-2 time-series in Figure 2 which is likely due to the European domain (see Figure S4 of the Supplement) extending to high northern latitudes (approximately 70°N) where sampling of the GOME-2 UV sounder, but not IASI, is restricted in winter months by absence of sunlight. While this could slightly influence the domain average annual cycle comparison it does not affect the interannual variability subject of this study.

Formatted: Font: (Default) Times New Roman, 10 pt, Not Italic

Formatted: Font: Italic

In 2022, the IASI-IMS-Extended record shows even larger negative anomalies in April and May than 2020/2021, of 2.6 DU (15.0%) and 2.8 DU (14.6%), respectively, which are well beyond the average ± 2σ threshold. The negative anomalies continue in June and July, with 1.3 DU (6.5%) and 1.3 DU (6.1%). In 2023, the negative anomalies in spring-summer are smaller compared to 2020–2022, apart from in May, where the negative anomaly is 1.3 DU (6.1%). Broadly, the years of 2020–2023 all show monthly anomalies which are more consistently negative than the previous 12 years. The question of the persistence of low European O_3 values will become evident in future years through extension of these MetOp records.

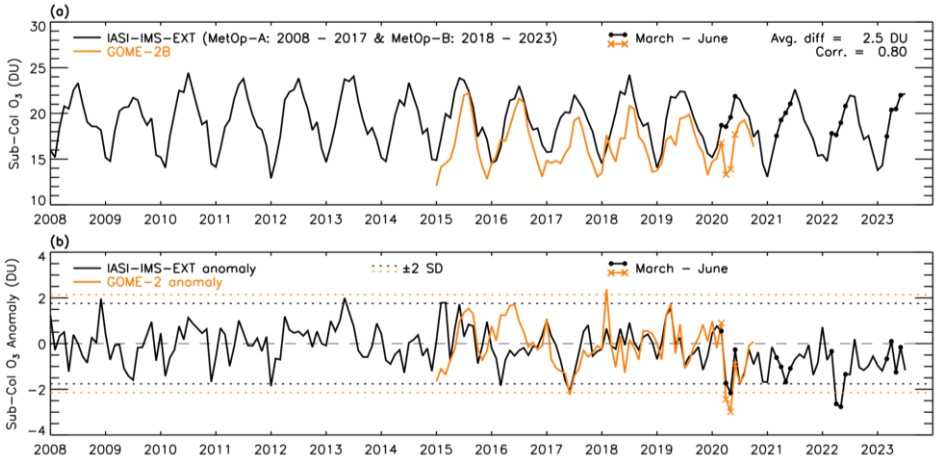

Figure 2. European satellite-derived O_3 from January 2008–July 2023. (a) Monthly average sub-column (surface–450 hPa) O_3 record (DU) from IASI (IASI-IMS-extended, January 2008–July 2023) and GOME-2B (January 2015–

October 2020). (b) Monthly mean anomalies for the two records (2015–2019 baseline for GOME-2B, 2008–2019 for IASI-IMS-Extended) (DU). Dotted lines indicate ± 2σ from the average of the record. Filled circles (IASI-IMS-Extended) and crosses (GOME-2B) are shown for the months of March–June in 2020–2023, to highlight the relevant spring/summer periods. Average difference and correlation are based on January 2015–December 2019.

3.2 TOMCAT Model Experiments (2017–2021)

In 2020, scaling the emissions according to the mobility data estimates in Forster et al. (2020) (TOMCAT COVID scenario) caused a monthly reduction in tropospheric O_3 from March to December (**Figure 3(a)**). During January and February, the COVID and BAU scenarios are very similar, however, from March onwards the COVID scenario shows a negative difference compared to the BAU scenario, which peaks at 2.0 DU (8.3%) lower in May. This negative difference then reduces through the year to December (0.7 DU, 4.1%). **Figure 4a** shows the spatial impact of COVID-19 on lower troposphere ozone simulated by TOMCAT. The March-May 2020 average is typically 1.0-2.0 DU lower across the whole European domain. In 2021, the COVID scenario in Figure 3(a) shows consistent reductions in all months of the year, starting at 0.6 DU (3.4%) in January, peaking at 1.0 DU (4.3%) in May, and reducing towards the end of the year, ending with 0.6 DU (3.2%) in December. The temporal pattern of the reduction is similar to that in surface emissions (**Figure 1**), although with considerably smaller percentage decreases (peak of ~30% for surface emissions and ~8% for the resulting O_3 sub-column). This highlights the large emission reductions required for a sizeable reduction in European lower tropospheric O_3. To identify the impact of meteorology in 2020, the scaled emissions in 2020 were used in three separate simulations with the meteorology of 2017, 2018 and 2019, with an average of these three scaled emission simulations shown in **Figure 3(b)**. The 2020 COVID scenario record is broadly lower than the 2017/2018/2019 averaged scaled emission scenario, despite using the same surface emissions, which indicates that the meteorology of 2020 had a large impact on the tropospheric O_3 reduction. Here, we use the term "meteorology" to represent meteorological variables such as temperature, pressure and humidity, but also the long-range transport (i.e. advection/convection) of air masses, which influence tropospheric chemistry. This is supported by **Figure 4b** which shows that across most of Europe, 2020 meteorological conditions where more conducive to lower tropospheric ozone loss (i.e. differences of -3.0 and -1.0 DU) than previous years. However, the domain average shown for March-May 2020 in **Figure 3b** is buffered by the positive differences (up to 1.0-1.5 DU) above 60°*N*. The impact of meteorology in 2020 is greatest in the spring-summer (**Figure 3b**), as the differences between these two timeseries is largest from February–July, peaking at a 1.1 DU difference in May. This demonstrates the importance of meteorology to the resulting O_3 in the spring-summer of 2020. The records are much more consistent from August to the end of the year, with absolute differences below 0.6 DU, indicating a reduced impact from meteorology in the second half of the year.

~~In 2020, scaling the emissions according to the mobility data estimates in Forster et al. (2020) (TOMCAT COVID scenario) caused a monthly reduction in tropospheric O_3 from March to December (**Figure 3(a)**). During January and February, the COVID and BAU scenarios are very similar, however, from March onwards the COVID scenario shows a negative difference compared to the BAU scenario, which peaks at 2.0 DU (8.3%) lower in May. This negative difference then reduces through the year to December (0.7 DU, 4.1%). In 2021, the COVID scenario shows consistent reductions in all months of the year, starting at 0.6 DU (3.4%) in January, peaking at 1.0 DU (4.3%) in May, and getting slightly smaller towards the end of the year, ending with 0.6 DU (3.2%) in December. The temporal pattern of the reduction is similar to the reduction in surface emissions (**Figure 1**), although with much smaller percentage decreases (peak of ~30% for surface emissions and ~8% for the resulting O_3 sub-column). This highlights the large emission reductions required for a sizeable reduction in European tropospheric O_3.~~

~~To identify the impact of meteorology in 2020, the scaled emissions in 2020 were used in three separate simulations with the meteorology of 2017, 2018 and 2019, with an average of these three scaled emission simulations shown in **Figure 3(b)**. The 2020 COVID scenario record is broadly lower than the 2017/2018/2019 averaged scaled emission scenario, despite using the same surface emissions, which indicates that the meteorology of 2020 had a large impact~~

Formatted: Font: 10 pt

Formatted: Font: (Default) Times New Roman, 10 pt

~~on the tropospheric O_3 reduction. The impact of meteorology in 2020 is greatest in the spring-summer, as the differences between these two timeseries is largest from February–July, peaking at a 1.1 DU difference in May. This demonstrates the importance of meteorology to the resulting O_3 in the spring-summer of 2020. The records are much more consistent from August to the end of the year, with absolute differences below 0.6 DU, indicating a reduced impact from meteorology in the second half of the year.~~

In comparison with the previous 3 years (2017–2019), the BAU scenario in 2020 and 2021 has lower peak spring-summer values of O_3, especially compared to the high O_3 values in 2019 (**Figure 3(a)**). The spring-summer of 2020 shows negative anomalies in the BAU scenario of up to 1.4 DU (-5.8%) (**Figure 3(c)**). April, May and July show the largest reductions, which are around the value of the average ± 2σ threshold (± 1.3 DU, 6.2%). The spring-summer BAU scenario reductions are repeated in 2021 from January–June, peaking at 1.2 DU (4.9%) in May. Any variation in the BAU scenario is due to meteorology and also variation in the BAU surface emissions used. As shown in **Figure 1**, the BAU emissions only vary by a small amount from year to year, e.g. the average total annual anthropogenic emission difference between consecutive years across the simulation time period is 0.33 Tg (2.0%) for NO_x, 1.3 Tg (4.4%) for CO and 0.06 Tg (1.8%) for VOCs. With consistent BAU emissions, meteorology is the dominant control in the BAU scenario and had a large impact on the simulated tropospheric O_3 in the spring and summer of 2020.

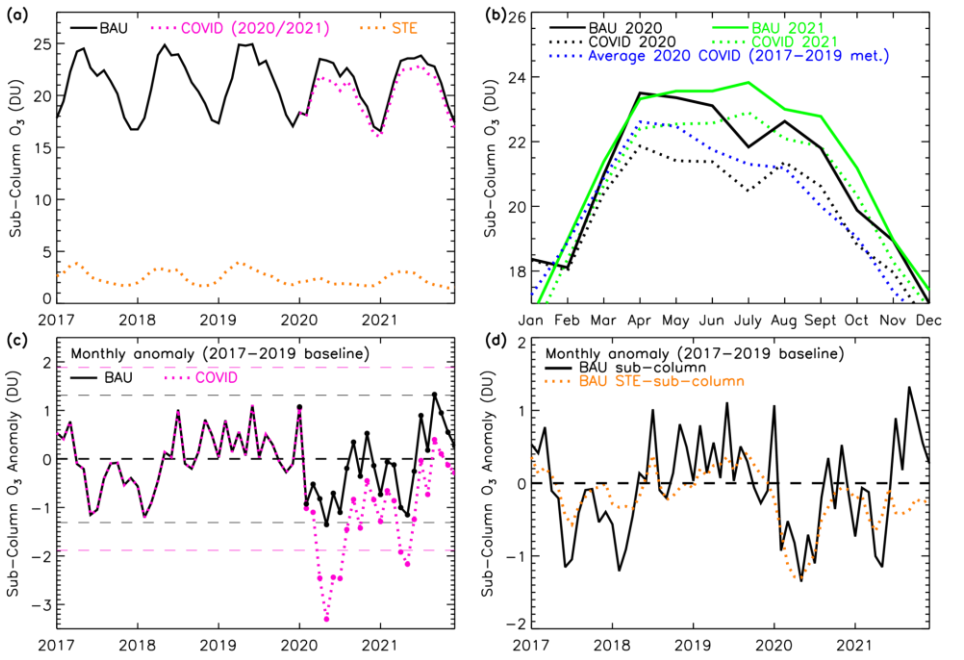

Figure 3. TOMCAT European lower tropospheric sub-column O_3 (surface–450 hPa) between 2017 and 2021 (DU). (a) Monthly sub-column O_3 averages for the BAU sub-column (solid, black) and STE-contribution sub-column (dotted, orange). The COVID scenario is shown in 2020 and 2021 (pink dotted). (b) BAU (solid, black) and COVID scenario (dotted) records for 2020 (black), 2021 (green), with the 2017/2018/2019 averaged COVID scenario (2020 scaled emissions, dark blue, dotted). (c) BAU (solid, black) and COVID (pink, dotted) O_3 anomalies (baseline of 2017–2019). Horizonal dashed lines indicate ± 2σ from the average of the record. (d) As panel (c) with the inclusion of monthly O_3 anomalies of the stratosphere-troposphere exchange (STE)-contribution sub-column (orange, dotted).

The COVID scenario shows large negative anomalies in 2020, peaking at 3.3 DU (15.4%) in May 2020 (**Figure 3c**), which is much more than the average ± 2σ threshold (± 1.9 DU, 9.0%). Comparing the BAU and COVID scenarios suggests that ~1 DU of the negative anomaly is due to meteorology (and small variations in BAU emissions) and the remaining contribution (~ 1–2 DU in spring-summer) of the negative anomaly is due to the scaled emissions for 2020. The contribution of O_3 from STE to the troposphere in the model sub-column is calculated by TOMCAT as a tracer which represents stratospheric O_3 that has entered the troposphere and is controlled by tropospheric sink processes. We calculate a sub-column based on this contribution (STE-sub-column), shown in **Figure 3(a)**, varying between 1.5–4.0 DU from 2017–2021. We find a large negative anomaly in model stratosphere-troposphere O_3 exchange (STE) in the spring-summer of 2020 (**Figure 3(d)**), of 1.3 DU in both April and May (52.5% and 60.5%, respectively). The STE-sub-column absolute negative anomaly is a similar value or larger than the lower tropospheric sub-column anomaly from March - August in 2020, suggesting that during this period, low STE contribution was a substantial factor in the BAU scenario lower tropospheric sub-column O_3 reduction. In the months where the STE-sub-column absolute anomaly is larger than the BAU anomaly, the other controlling factors in the BAU simulation O_3 are likely around neutral or even slightly positive. The stratospheric O_3 used in the model simulation is a climatology, therefore, any variation on the STE contribution is from variation in the STE flux. In 2021, the negative anomaly in STE-sub-column is smaller than for 2020, reaching a peak value of 0.7 DU (21.5%) in April (**Figure 3(d)**). The STE-sub-column negative anomaly is also not larger than for the lower tropospheric sub-column in 2021, suggesting that the STE reduction had a smaller impact on the negative lower tropospheric sub-column anomalies seen in 2021, in comparison with 2020.

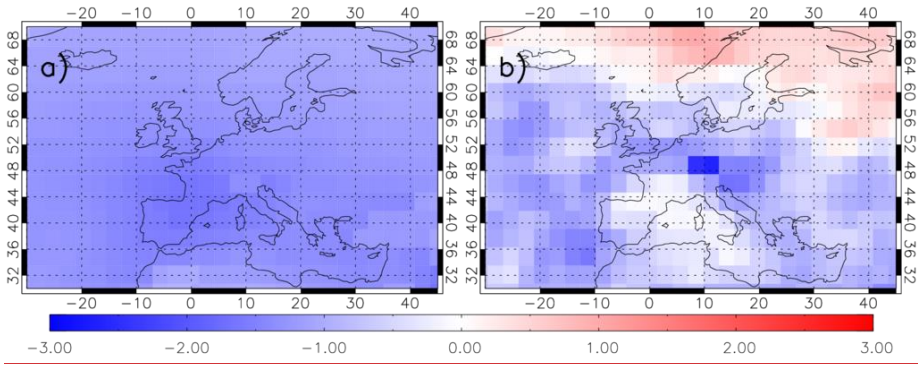

Figure 4: TOMCAT lower tropospheric ozone (DU) differences (March-May 2020 average) between a) the TOMCAT COVID and TOMCAT BAU simulations and b) the TOMCAT COVID simulation with 2017-2019 average meteorology (TOMCAT run for 2017, 2018 and 2019 with 2020 COVID emissions and the three simulations averaged together) and the TOMCAT BAU simulation.

Formatted: Font: (Default) Times New Roman, 10 pt

To further quantify the relative contributions, the difference between the anomalies for the BAU and COVID scenario as a relative percentage of the COVID scenario for 2020 (i.e. 100 × (BAU - COVID)/COVID) is shown in **Figure 45(a)**. We performed this quantification for spring-summer months showing a negative anomaly in both scenarios (March–August 2020 and March–June 2021). These values represent the percentage contributions of the emission reductions (due to COVID-19) and meteorological conditions to the determined reduction in the lower tropospheric column zone. ~~These values represent the contribution of the emission reduction to the negative anomalies seen in the COVID scenario, and the corresponding contribution of meteorology (and small differences in the BAU emissions).~~ The contribution of emissions to the COVID scenario in spring-summer 2020 is 53% (March), 67% (April), 59% (May), 71% (June), 55% (July) and 87% (August), with an average of 65% across these months. Therefore, scaling the emissions is the dominant influence during this period. In 2021, the COVID scenario also shows large negative anomalies, peaking at 2.2 DU (9.6%) in May. Scaling the emissions contributed towards 86%, 48%, 47% and 80% for March–June, respectively, of the scaled negative anomaly (average of 65%), with the rest due to meteorology (and BAU emissions).

Formatted: Font: (Default) Times New Roman, 10 pt

~~The contribution of O_3 from STE to the troposphere in the model sub-column is calculated by TOMCAT as a tracer which represents stratospheric O_3 that has entered the troposphere and is controlled by tropospheric sink processes. We calculate a sub-column based on this contribution (STE-sub-column), shown in **Figure 3(a)**, varying between 1.5–4.0 DU from 2017–2021. We find a large negative anomaly in model stratosphere-troposphere O_3 exchange (STE) in the spring-summer of 2020 (**Figure 3(d)**), of 1.3 DU in both April and May (52.5% and 60.5%, respectively). The STE sub-column absolute negative anomaly is a similar value or larger than the lower tropospheric sub-column anomaly from March – August in 2020, suggesting that during this period, low STE contribution was a substantial factor in the BAU scenario lower tropospheric sub-column O_3 reduction. In the months where the STE sub-column absolute anomaly is larger than the BAU anomaly, the other controlling factors in the BAU simulation O_3 are likely around neutral or even slightly positive. The stratospheric O_3 used in the model simulation is a climatology, therefore, any variation on the STE contribution is from variation in the STE flux. In 2021, the negative anomaly in STE-sub-column is smaller than for 2020, reaching a peak value of 0.7 DU (21.5%) in April (**Figure 3(d)**). The STE-sub-column negative anomaly is also not larger than for the lower tropospheric sub-column in 2021, suggesting that the STE reduction had a smaller impact on the negative lower tropospheric sub-column anomalies seen in 2021, in comparison with 2020.~~

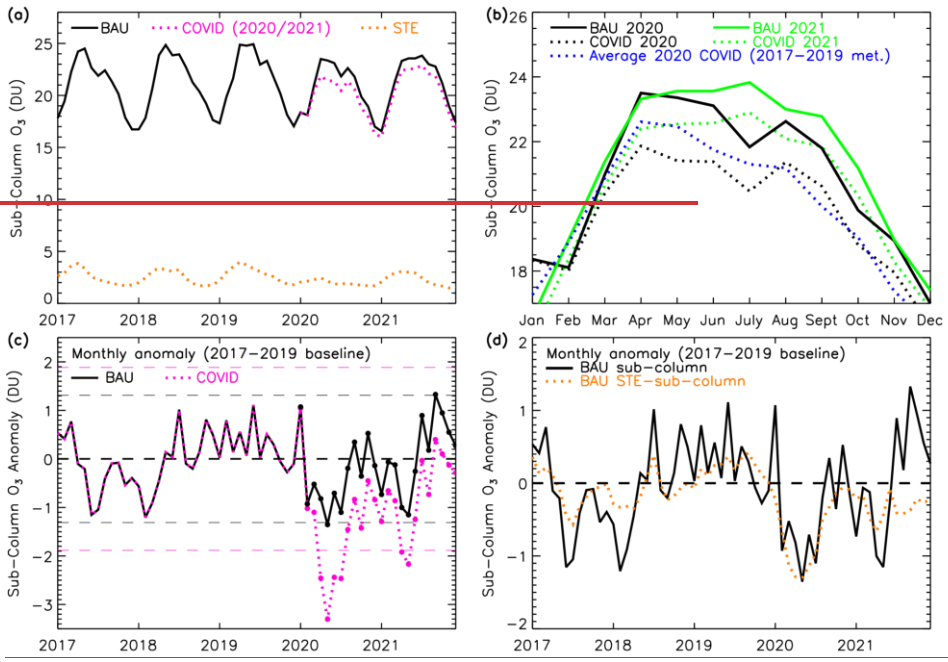

Figure 3. TOMCAT European lower tropospheric sub-column O_3 (surface–450 hPa) between 2017 and 2021 (DU). (a) Monthly sub-column O_3 averages for the BAU sub-column (solid, black) and STE-contribution sub-column (dotted, orange). The COVID scenario is shown in 2020 and 2021 (pink dotted). (b) BAU (solid, black) and COVID scenario (dotted) records for 2020 (black), 2021 (green), with the 2017/2018/2019 averaged COVID scenario (2020 scaled emissions, dark blue, dotted). (c) BAU (solid, black) and COVID (pink, dotted) O_3 anomalies (baseline of 2017–2019). Horizonal dashed lines indicate ± 2σ from the average of the record. (d) As panel (c) with the inclusion of monthly O_3 anomalies of the STE-contribution sub-column (orange, dotted).

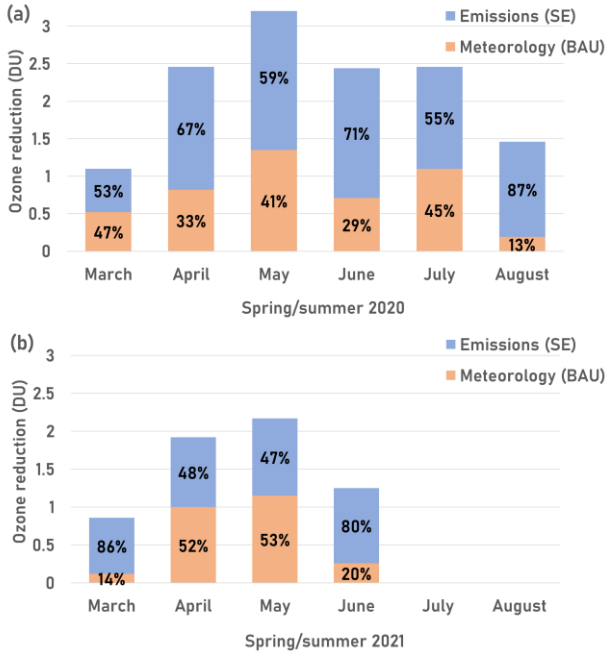

Figure 45. Contribution of scaled emissions and meteorology/BAU emissions to the TOMCAT lower tropospheric sub-column O_3 reduction from March–August in (a) 2020 and (b) 2021. The total reduction (DU) is the COVID scenario negative anomaly, with the relative contribution of meteorology/BAU emissions shown in orange and the contribution of scaled emissions shown in blue. The percentage relative contribution is labelled onto each bar section.

4 Conclusions

Our study represents one of the first extended investigations of the COVID-19 pandemic impacts on European lower tropospheric O_3 (surface-450 hPa) using satellite observations and modelling. The records from the Global Ozone Monitoring Experiment (GOME – 2) and the Infrared Atmospheric Sounding Interferometer (IASI) on MetOp-B show substantial decreases in European average spring-summer time lower tropospheric ozone of typically 2.0-3.0 DU (or 11.0-14.6%). While not the key focus of this paper, the 2022 decline in O_3 is interestingly the largest between 2020 and 2023. Therefore, this would suggest other factors not investigated in this study are driving a more substantial O_3 decrease and that the reported COVID-19 response is within the more extreme variability of European ozone.

To investigate the drivers of the O_3 decreases over Europe during the COVID-19 period (2020-2021), activity scaling factors (i.e. based on anonymised mobility data from big tech firms) were used to perturb the model's business-as-usual (BAU) emissions for 2020 and 2021 to quantify the COVID-19 impact on O_3. Here, the TOMCAT simulations of lower tropospheric O_3 were reduced by 2.0-3.0 DU (comparable to the O_3 reductions reported by the satellite records) in the COVID-19 simulation compared to the BAU baseline. Further model sensitivity experiments were able to diagnose the contribution of 2020 emissions changes (approximately 66%) and 2020 meteorological conditions (approximately 34%) to the overall TOMCAT simulated O_3 reduction in Europe. Therefore, the COVID-19 reduced in O_3 precursor emissions were substantial in reducing 2020 European O_3, but it

Formatted: Font: 10 pt

Formatted: Font: (Default) Times New Roman, 10 pt

Formatted: Font: (Default) Times New Roman, 10 pt, Not Italic

Formatted: Font: (Default) Times New Roman, 10 pt

Formatted: Font: (Default) Times New Roman, 10 pt, Not Italic

was amplified by meteorological conditions that year. Investigation of the TOMCAT stratospheric O_3 tagged tracer (i.e. a representation of the flux of stratospheric rich O_3 air into the troposphere) suggested a substantial drop in its contribution to lower tropospheric O_3 (in the order of 1.0 DU), which was comparable to the meteorological signal. Thus, a likely cause of the amplified European O_3 reduction in the COVID-19 period. Therefore, our study has successfully quantified the impact of COVID-19 on European lower tropospheric ozone and identified a useful methodology to isolate the impact of emission changes, but also importantly meteorological variability, on observed changes in tropospheric composition. Future work would focus on the large reduction in European O_3 in 2022 (which is beyond the scope of this study), produce a harmonised IASI O_3 record from the three MetOp satellites and a reprocessing of the RAL Space GOME-2 record to more accurately account for UV-degradation in the instrument record. ~~Our study represents the first extended investigation of the COVID-19 pandemic impacts on European lower tropospheric O_3 (surface-450 hPa) up to mid-2023. Satellite records show a substantially prolonged European average decrease in spring-summer lower tropospheric in 2020, 2021 and 2022 (and to a lesser extent in 2023) peaking at ~ 1.5–3.0 DU. Modelled reductions, using scaled emissions in the TOMCAT CTM to account for changes in precursor trace gas emissions, are consistent for 2020 and 2021. The simulations showed that in April/May 2020, ~2/3 of the negative anomaly could be attributed to scaling the emissions, with the remaining reduction being attributed to meteorological processes; largely through a reduction in the flux of stratospheric O_3 into the troposphere. Further investigation is required to quantify the drivers of the large 2022 reductions in tropospheric O_3, which could be meteorological variability and/or the stabilisation of emissions below pre-2020 levels (i.e. a new normal in human activity post-COVID).~~

Acknowledgements

This work was funded by the UK Natural Environment Research Council (NERC) by providing funding for the National Centre for Earth Observation (NCEO, award reference NE/R016518/1) and the NERC Panorama Doctoral Training Programme (DTP, award reference 580 NE/S007458/1). The TOMCAT runs were undertaken on ARC3, part of the High-Performance Computing facilities at the University of Leeds, UK.

Data Availability

The IASI-IMS and GOME-2 data is available via the NERC Centre for Environmental Data Analysis (CEDA) Jasmin platform subject to data requests. However, the IASI-IMS data and TOMCAT simulations used in this study are available on Zenodo at https://zenodo.org/records/10424302 (Pimlott et al., 2024).

Author Contributions

MAP and RJP conceptualised, planned and undertook the research study. BJK, RS, BGL and LJV provided the data and advice on using the products. MAP performed the TOMCAT model simulations with support from MPC and WF. MAP prepared the manuscript with contributions from all co-authors.

Conflicts of Interest

The authors declare no conflicts of interest.

Formatted: Font: (Default) Times New Roman, 10 pt

Formatted: Font: (Default) Times New Roman, 10 pt, Not Italic

Formatted: Font: (Default) Times New Roman, 10 pt

Formatted: Font: 10 pt

Formatted: Font: 10 pt

Formatted: Font: 10 pt

Formatted: Font: 10 pt

References

Bouarar, I., Gaubert, B., Brasseur, G. P., Steinbrecht, W., Doumbia, T., Tilmes, S., et al. (2021). Ozone Anomalies in the Free Troposphere During the COVID-19 Pandemic. *Geophysical Research Letters*, *48*(16), 1–11. https://doi.org/10.1029/2021GL094204

Callies, J., Corpaccioli, E., Eisinger, M., Hahne, A., & Lefebvre, A. (2000). GOME-2-Metop's second-generation sensor for operational ozone monitoring. *ESA Bulletin*, *102*(may), 28–36.

Chang, K. L., Cooper, O. R., Gaudel, A., Allaart, M., Ancellet, G., Clark, H., et al. (2022). Impact of the COVID-19 Economic Downturn on Tropospheric Ozone Trends: An Uncertainty Weighted Data Synthesis for Quantifying Regional Anomalies Above Western North America and Europe. *AGU Advances*, *3*(2). https://doi.org/10.1029/2021AV000542

Chipperfield, M. P. (2006). New version of the TOMCAT/SLIMCAT off-line chemical transport model: Intercomparison of stratospheric tracer experiments. *Quarterly Journal of the Royal Meteorological Society*, *132*(617), 1179–1203. https://doi.org/10.1256/qj.05.51

Clark, H., Bennouna, Y., Tsivlidou, M., Wolff, P., Sauvage, B., Barret, B., et al. (2021). The effects of the COVID-19 lockdowns on the composition of the troposphere as seen by In-service Aircraft for a Global Observing System (IAGOS) at Frankfurt. *Atmospheric Chemistry and Physics*, *21*(21), 16237–16256. https://doi.org/10.5194/acp-21-16237-2021

Clerbaux, C., Boynard, A., Clarisse, L., George, M., Hadji-Lazaro, J., Herbin, H., et al. (2009). Monitoring of atmospheric composition using the thermal infrared IASI/MetOp sounder. *Atmospheric Chemistry and Physics*, *9*(16), 6041–6054. https://doi.org/10.5194/acp-9-6041-2009

Cuesta, J., Costantino, L., Beekmann, M., Siour, G., Menut, L., Bessagnet, B., et al. (2022). Ozone pollution during the COVID-19 lockdown in the spring of 2020 over Europe, analysed from satellite observations, in situ measurements, and models. *Atmospheric Chemistry and Physics*, *22*(7), 4471–4489. https://doi.org/10.5194/acp-22-4471-2022

Doumbia, T., Granier, C., Elguindi, N., Bouarar, I., Darras, S., Brasseur, G., et al. (2021). Changes in global air pollutant emissions during the COVID-19 pandemic: A dataset for atmospheric modeling. *Earth System Science Data*, *13*(8), 4191–4206. https://doi.org/10.5194/essd-13-4191-2021.

Dunn, R. J. H., J. Blannin, N. Gobron, J. B Miller, and K. M. Willett, Eds., 2024: Global Climate [in "State of the Climate in 2023"]. Bull. Amer. Meteor. Soc., 105 (8), S12–S155, https://doi.org/10.1175/BAMS-D24-0116.1.

European Environment Agency. (2022). *Air quality in Europe 2022*. https://doi.org/10.2800/488115

Feng, L., Smith, S. J., Braun, C., Crippa, M., Gidden, M. J., Hoesly, R., et al. (2020). The generation of gridded emissions data for CMIP6. *Geoscientific Model Development*, *13*(2), 461–482. https://doi.org/10.5194/gmd-13-461-2020

Formatted: Indent: Left: 0 cm, First line: 0 cm, Space After: 6 pt, Line spacing: Multiple 1.13 li, Widow/Orphan control, Adjust space between Latin and Asian text, Adjust space between Asian text and numbers

Feng, W., Dhomse, S. S., Arosio, C., Weber, M., Burrows, J. P., Santee, M. L., & Chipperfield, M. P. (2021). Arctic Ozone Depletion in 2019/20: Roles of Chemistry, Dynamics and the Montreal Protocol. *Geophysical Research Letters*, *48*(4), 1–10. https://doi.org/10.1029/2020GL091911

Forster, P. M., Forster, H. I., Evans, M. J., Gidden, M. J., Jones, C. D., Keller, C. A., et al. (2020). Current and future global climate impacts resulting from COVID-19. *Nature Climate Change*, *10*(10), 913–919. https://doi.org/10.1038/s41558-020-0883-0

Gidden, M. J., Riahi, K., Smith, S. J., Fujimori, S., Luderer, G., Kriegler, E., et al. (2019). Global emissions pathways under different socioeconomic scenarios for use in CMIP6: a dataset of harmonized emissions trajectories through the end of the century. *Geoscientific Model Development*, *12*(4), 1443–1475. https://doi.org/10.5194/gmd-12-1443-2019

Grange, S. K., Lee, J. D., Drysdale, W. S., Lewis, A. C., Hueglin, C., Emmenegger, L., & Carslaw, D. C. (2021). COVID-19 lockdowns highlight a risk of increasing ozone pollution in European urban areas. *Atmospheric Chemistry and Physics*, *21*(5), 4169–4185. https://doi.org/10.5194/acp-21-4169-2021

Guevara, M., Jorba, O., Soret, A., Petetin, H., Bowdalo, D., Serradell, K., et al. (2021). Time-resolved emission reductions for atmospheric chemistry modelling in Europe during the COVID-19 lockdowns. *Atmospheric Chemistry and Physics*, *21*(2), 773–797. https://doi.org/10.5194/acp-21-773-2021

Hersbach, H., Bell, B., Berrisford, P., Hirahara, S., Horányi, A., Muñoz-Sabater, J., et al. (2020). The ERA5 global reanalysis. *Quarterly Journal of the Royal Meteorological Society*, *146*(730), 1999–2049. https://doi.org/10.1002/qj.3803

IPCC. (2021). *Climate Change 2021: The Physical Science Basis: Contribution of Working Group I to the Sixth Assessment Report of the Intergovernmental Panel on Climate Change*. (V. Masson-Delmotte, P. Zhai, A. Pirani, S. L. Connors, C. Péan, S. Berger, et al., Eds.). Cambridge, United Kingdom: Cambridge University Press. https://doi.org/10.1017/9781009157896

Mann, G. W., Carslaw, K. S., Spracklen, D. V., Ridley, D. A., Manktelow, P. T., Chipperfield, M. P., et al. (2010). Description and evaluation of GLOMAP-mode: A modal global aerosol microphysics model for the UKCA composition-climate model. *Geoscientific Model Development*, *3*(2), 519–551. https://doi.org/10.5194/gmd-3-519-2010

Miles, G. M., Siddans, R., Kerridge, B. J., Latter, B. G., & Richards, N. A. D. (2015). Tropospheric ozone and ozone profiles retrieved from GOME-2 and their validation. *Atmospheric Measurement Techniques*, *8*(1), 385–398. https://doi.org/10.5194/amt-8-385-2015

Miyazaki, K., Bowman, K., Sekiya, T., Takigawa, M., Neu, J. L., Sudo, K., et al. (2021). Global tropospheric ozone responses to reduced NOx emissions linked to the COVID-19 worldwide

lockdowns. *Science Advances*, *7*(24), 1–15. https://doi.org/10.1126/sciadv.abf7460

Monks, P. S., Archibald, A. T., Colette, A., Cooper, O., Coyle, M., Derwent, R., et al. (2015). Tropospheric ozone and its precursors from the urban to the global scale from air quality to short-lived climate forcer. *Atmospheric Chemistry and Physics*, *15*(15), 8889–8973. https://doi.org/10.5194/acp-15-8889-2015

Monks, S. A., Arnold, S. R., Hollaway, M. J., Pope, R. J., Wilson, C., Feng, W., et al. (2017). The TOMCAT global chemical transport model v1.6: Description of chemical mechanism and model evaluation. *Geoscientific Model Development*. https://doi.org/10.5194/gmd-10-3025-2017

Munro, R., Lang, R., Klaes, D., Poli, G., Retscher, C., Lindstrot, R., et al. (2016). The GOME-2 instrument on the Metop series of satellites: Instrument design, calibration, and level 1 data processing - An overview. *Atmospheric Measurement Techniques*, *9*(3), 1279–1301. https://doi.org/10.5194/amt-9-1279-2016

Ordóñez, C., Garrido-Perez, J. M., & García-Herrera, R. (2020). Early spring near-surface ozone in Europe during the COVID-19 shutdown: Meteorological effects outweigh emission changes. *Science of the Total Environment*, *747*(December 2019), 141322. https://doi.org/10.1016/j.scitotenv.2020.141322

Parrish, D. D., Derwent, R. G., Faloona, I. C., & Mims, C. A. (2022). Technical note: Northern midlatitude baseline ozone - Long-term changes and the COVID-19 impact. *Atmospheric Chemistry and Physics*, *22*(20), 13423–13430. https://doi.org/10.5194/acp-22-13423-2022

Pey, J., & Cerro, J. C. (2022). Reasons for the observed tropospheric ozone weakening over south-western Europe during COVID-19: Strict lockdown versus the new normal. *Science of the Total Environment*, *833*(March). https://doi.org/10.1016/j.scitotenv.2022.155162

Pimlott, M. A., Pope, R. J., Kerridge, B. J., Siddans, R., Latter, B. G., Ventress, L. J., et al. (2024). TOMCAT model data & IASI/GOME-2B satellite data of European ozone between 2008 - 2023. Zenodo. https://doi.org/doi.org/10.5281/zenodo.10424302

Pope, R. J., Arnold, S. R., Chipperfield, M. P., Reddington, C. L. S., Butt, E. W., Keslake, T. D., et al. (2020). Substantial increases in Eastern Amazon and Cerrado biomass burning-sourced tropospheric ozone. *Geophysical Research Letters*, 47, e2019GL084143. https://doi.org/10.1029/2019GL084143.

Pope, R J, Kerridge, B. J., Chipperfield, M. P., Siddans, R., Latter, B. G., Ventress, L. J., et al. (2023). Investigation of the summer 2018 European ozone air pollution episodes using novel satellite data and modelling. *Atmospheric Chemistry and Physics*, *23*(20), 13235–13253. https://doi.org/10.5194/acp-23-13235-2023

Pope, Richard J., Kerridge, B. J., Siddans, R., Latter, B. G., Chipperfield, M. P., Arnold, S. R., et al. (2021). Large enhancements in southern hemisphere satellite-observed trace gases due to the

Formatted: Indent: Left: 0 cm, First line: 0 cm, Space After: 6 pt, Line spacing: Multiple 1.13 li, Widow/Orphan control, Adjust space between Latin and Asian text, Adjust space between Asian text and numbers

Formatted: Font: (Default) +Body (Calibri), Font color: Red, Check spelling and grammar

2019/2020 Australian wildfires. *Journal of Geophysical Research: Atmospheres*, 1–13. https://doi.org/10.1029/2021jd034892

Pope, R. J., Rap, A., Pimlott, M. A., Barret, B., Le Flochmoen, E., Kerridge, B. J., Siddans, R., Latter, B. G., Ventress, L. J., Boynard, A., Retscher, C., Feng, W., Rigby, R., Dhomse, S. S., Wespes, C., and Chipperfield, M. P.: Quantifying the tropospheric ozone radiative effect and its temporal evolution in the satellite era, Atmos. Chem. Phys., 24, 3613–3626, https://doi.org/10.5194/acp-24-3613-2024, 2024.

Putero, D., Cristofanelli, P., Chang, K.-L., Dufour, G., Beachley, G., Couret, C., Effertz, P., Jaffe, D. A., Kubistin, D., Lynch, J., Petropavlovskikh, I., Puchalski, M., Sharac, T., Sive, B. C., Steinbacher, M., Torres, C., and Cooper, O. R.: Fingerprints of the COVID-19 economic downturn and recovery on ozone anomalies at high-elevation sites in North America and western Europe, Atmos. Chem. Phys., 23, 15693–15709, https://doi.org/10.5194/acp-23-15693-2023, 2023.

Riahi, K., van Vuuren, D. P., Kriegler, E., Edmonds, J., O'Neill, B. C., Fujimori, S., et al. (2017). The Shared Socioeconomic Pathways and their energy, land use, and greenhouse gas emissions implications: An overview. *Global Environmental Change*, *42*, 153–168. https://doi.org/https://doi.org/10.1016/j.gloenvcha.2016.05.009

Richards, N. A. D., Arnold, S. R., Chipperfield, M. P., Miles, G., Rap, A., Siddans, R., et al. (2013). The Mediterranean summertime ozone maximum: Global emission sensitivities and radiative impacts. *Atmospheric Chemistry and Physics*, *13*(5), 2331–2345. https://doi.org/10.5194/acp-13-2331-2013.

Rowlinson, M. J., Rap, A., Arnold, S. R., Pope, R. J., Chipperfield, M. P., McNorton, J., Forster, P., Gordon, H., Pringle, K. J., Feng, W., Kerridge, B. J., Latter, B. L., and Siddans, R.: Impact of El Niño–Southern Oscillation on the interannual variability of methane and tropospheric ozone, Atmos. Chem. Phys., 19, 8669–8686, https://doi.org/10.5194/acp-19-8669-2019, 2019.

Skeie, R. B., Myhre, G., Hodnebrog, Ø., Cameron-Smith, P. J., Deushi, M., Hegglin, M. I., et al. (2020). Historical total ozone radiative forcing derived from CMIP6 simulations. *Npj Climate and Atmospheric Science*, *3*(1). https://doi.org/10.1038/s41612-020-00131-0

Spracklen, D. V., Pringle, K. J., Carslaw, K. S., Chipperfield, M. P., & Mann, G. W. (2005). A global off-line model of size-resolved aerosol microphysics: I. Model development and prediction of aerosol properties. *Atmospheric Chemistry and Physics*, *5*(8), 2227–2252. https://doi.org/10.5194/acp-5-2227-2005

Steinbrecht, W., Kubistin, D., Plass-Dülmer, C., Davies, J., Tarasick, D. W., Von Der Gathen, P., et al. (2021). COVID-19 Crisis Reduces Free Tropospheric Ozone Across the Northern Hemisphere. *Geophysical Research Letters*, *48*(5), 1–11. https://doi.org/10.1029/2020GL091987

Weber, M., Arosio, C., Feng, W., Dhomse, S. S., Chipperfield, M. P., Meier, A., et al. (2021). The Unusual Stratospheric Arctic Winter 2019/20: Chemical Ozone Loss From Satellite Observations and TOMCAT Chemical Transport Model. *Journal of Geophysical Research: Atmospheres*, *126*(6), 1–14. https://doi.org/10.1029/2020JD034386

Formatted: Indent: Left: 0 cm, First line: 0 cm, Space After: 6 pt, Line spacing: Multiple 1.13 li, Widow/Orphan control, Adjust space between Latin and Asian text, Adjust space between Asian text and numbers

Formatted: Indent: Left: 0 cm, First line: 0 cm, Space After: 6 pt, Line spacing: Multiple 1.13 li, Widow/Orphan control, Adjust space between Latin and Asian text, Adjust space between Asian text and numbers

Formatted: Font: (Default) +Body (Calibri), Font color: Red, Check spelling and grammar

WHO. (2020). Naming the coronavirus disease (COVID-19) and the virus that causes it. Retrieved April 14, 2023, from https://www.who.int/emergencies/diseases/novel-coronavirus-2019/technical-guidance/naming-the-coronavirus-disease-(covid-2019)-and-the-virus-that-causes-it

Wohltmann, I., von der Gathen, P., Lehmann, R., Maturilli, M., Deckelmann, H., Manney, G. L., et al. (2020). Near-Complete Local Reduction of Arctic Stratospheric Ozone by Severe Chemical Loss in Spring 2020. *Geophysical Research Letters*, *47*(20). https://doi.org/10.1029/2020GL089547

Young, P. J., Archibald, A. T., Bowman, K. W., Lamarque, J.-F., Naik, V., Stevenson, D. S., Tilmes, S., Voulgarakis, A., Wild, O., Bergmann, D., Cameron-Smith, P., Cionni, I., Collins, W. J., Dalsøren, S. B., Doherty, R. M., Eyring, V., Faluvegi, G., Horowitz, L. W., Josse, B., Lee, Y. H., MacKenzie, I. A., Nagashima, T., Plummer, D. A., Righi, M., Rumbold, S. T., Skeie, R. B., Shindell, D. T., Strode, S. A., Sudo, K., Szopa, S., and Zeng, G.: Pre-industrial to end 21st century projections of tropospheric ozone from the Atmospheric Chemistry and Climate Model Intercomparison Project (ACCMIP), Atmos. Chem. Phys., 13, 2063–2090, https://doi.org/10.5194/acp-13-2063-2013, 2013.

Zhou, P., Yang, X. Lou, Wang, X. G., Hu, B., Zhang, L., Zhang, W., et al. (2020). A pneumonia outbreak associated with a new coronavirus of probable bat origin. *Nature*, *579*(7798), 270–273. https://doi.org/10.1038/s41586-020-2012-7

Ziemke, J. R., Kramarova, N. A., Frith, S. M., Huang, L. K., Haffner, D. P., Wargan, K., et al. (2022). NASA Satellite Measurements Show Global-Scale Reductions in Free Tropospheric Ozone in 2020 and Again in 2021 During COVID-19. *Geophysical Research Letters*, *49*(15). https://doi.org/10.1029/2022GL098712

Formatted: Indent: Left: 0 cm, First line: 0 cm, Space After: 6 pt, Line spacing: Multiple 1.13 li, Widow/Orphan control, Adjust space between Latin and Asian text, Adjust space between Asian text and numbers

Formatted: Font: (Default) +Body (Calibri), Font color: Red, Check spelling and grammar